Cancer growth: Predictions of a realistic model

S. A. Menchón* and C. A. Condat
CONICET and FaMAF, Universidad Nacional de Córdoba, 5000-Córdoba, Argentina
(Received 25 April 2008; published 8 August 2008)

Simulations of avascular cancer growth are performed using experimental values of the relevant parameters. This permits a realistic assessment of the influence of these parameters on cancer growth dynamics. In general, an early exponential growth phase is followed by a linear regime (as observed in recent experiments), while the thickness of the viable cell layer remains approximately constant. Contrary to some predictions, a transition to latency is not observed.

DOI: 10.1103/PhysRevE.78.022901 PACS number(s): 87.17.Aa, 87.17.Ee, 87.18.Hf

The complexity of tumor dynamics is such that it would be impractical to try to formulate a mathematical model that embodies all the relevant processes. However, sophisticated mathematical models have been put forward to examine the influence of various mechanisms at different growth stages [1–6]. The competition for nutrients is a crucial growth-controlling factor. On this basis, a model was proposed a few years ago to describe the possible morphologies of avascular tumor growth [7]. Starting from a consistent set of rules for the cellular interactions, a set of coupled nonlinear iteration equations was formulated and solved by direct numerical simulation. This model has led not only to various realistic morphologies, but also to the prediction of a phase transition from growth to latency [8], to a description of the dynamics of tumor cords [9], and to an analysis of how anatomical constraints condition tumor growth [10]. More recently, it has been used to describe some aspects of the tumor-immune system interaction [11] and the shedding of cells by multicellular tumor spheroids (MTSs) [12]. Of course, the detailed predictions of the model depend on the values chosen for the parameters. In Ref. [7], the parameters were given arbitrary (though reasonable) values. Nowadays, since much more is known about the experimental values of the parameters, we can make our predictions far more precise. In this Brief Report we use the model of Scalerandi and co-workers to predict some key properties of a growing avascular tumor. For instance, there have been controversies about the law controlling the growth of the total tumor mass, the more traditional view stating that it is well described by the Gompertz law [2,5] and new research indicating that power laws give better descriptions [13,14]. Our simulations help to clarify this problem by precisely predicting what can be expected on the basis of the model hypotheses. We also address the problem of the existence of a phase transition from tumor growth to latency, finding that this transition does not occur when realistic parameter values are used.

In the model of Ref. [7] the tissue is represented by a network whose node points are each associated with a volume element that contains many cells and nutrient molecules. Healthy, cancerous, and dead cells coexist at each node point, their concentrations being, respectively, $h(\vec{i})$, $c(\vec{i})$, and $d(\vec{i})$. The total cell concentration is considered to be uniform and normalized.

The nutrient that diffuses through the tissue is called free nutrient. For simplicity, we consider a single critical nutrient—i.e., glucose—whose concentration and diffusion coefficient will be denoted by $p(\vec{i},t)$ and α', respectively. The rules governing the behavior of the cancer cells are the following.

(i) *Feeding*. Cancer cells absorb free nutrients at the rate

$$\gamma(\vec{i}) = \gamma_{as}(1 - e^{-\Gamma p(\vec{i})}), \tag{1}$$

where Γ is an affinity parameter, which we will take equal to unity. The absorption rate is proportional to the local free nutrient concentration $p(\vec{i})$ at low concentrations, but it saturates (to γ_{as}) at high concentrations. Absorbed nutrients are called bound nutrients.

(ii) *Consumption*. The bound nutrient, whose concentration is $q(\vec{i})$, is consumed by cancer cells at the rate

$$\beta(\vec{i}) = \beta_{as}(1 - e^{-q(\vec{i})/c(\vec{i})}), \tag{2}$$

where the denominator $c(\vec{i})$ has been included in the exponent because each cell can consume only its own bound nutrient.

(iii) *Death*. When the average amount of bound nutrient per cell, $q(\vec{i})/c(\vec{i})$, falls below a given threshold Q_D, a fraction $r_D c(\vec{i})$ of cancer cells dies.

(iv) *Mitosis*. A high concentration of bound nutrient may trigger cell replication. This is supposed to occur if $q(\vec{i})/c(\vec{i})$ exceeds a mitosis threshold Q_M $(Q_M > Q_D)$; in this time, a fraction $f_{i,j}$ of healthy cells is transformed into cancer cells. The fraction $f_{i,j}$ is given by

$$f_{i,j} = h(\vec{i}) + [r_M c(\vec{i}) - h(\vec{i})]\Theta(h(\vec{i}) - r_M c(\vec{i})), \tag{3}$$

where Θ is Heaviside's step function and r_M is a constant.

(v) *Migration*. A cell that senses a low nutrient level in its neighborhood tends to migrate. We assume that it moves with a migration rate α if $p(\vec{i})/c(\vec{i}) < P_D$, where P_D is the migration threshold. Since healthy cells are less mobile and aggressive than cancer cells, we assume that they are eliminated when cancer cells arrive, in such a way that the total cell concentration is preserved.

Implementation of these rules generates a system of coupled nonlinear iteration equations which is detailed in Ref. [7]. As an example, we write the iteration equation for

*menchon@famaf.unc.edu.ar

the evolution of the free nutrient concentration:

$$p(\vec{i},t+\tau) = p(\vec{i},t) + \tau\left\{ \sum_{\vec{i}'} \frac{\alpha'}{\ell^2}[p(\vec{i}',t) - p(\vec{i},t)] - \gamma_0 p(\vec{i},t)h(\vec{i},t) - \gamma(\vec{i},t)c(\vec{i},t) \right\}, \quad (4)$$

where τ is the iteration interval and γ_0 the healthy cell nutrient absorption coefficient. The first term inside the curly brackets corresponds to nutrient diffusion to and from the nearest neighbors of $\vec{i}$, and the second and third terms correspond, respectively, to healthy and cancer cells absorption.

We represent the tissue of interest by a two-dimensional square grid, with lattice constant ℓ and node points $\vec{i} = (\ell i; \ell j)$, where i and j are integers. The nutrients are supplied by a single capillary vessel situated at the lower edge of the lattice. The nutrient concentration in the blood vessel is constant, $p((\ell i;0),t) = P_0$. Periodic boundary conditions are used for the left and right boundaries. Initially we consider a healthy tissue with stationary nutrient distribution. In the *local interaction simulation approach* of Scalerandi *et al.* [7], the cellular and nutrient concentrations are modified by the local conditions at each step. In this work we use an improved implementation to minimize numerical errors.

Our two-dimensional square grid represents a slab of tissue of size 1 cm $\times$ 1 cm. If we consider a lattice with 300×300 node points, then $\ell \approx 33$ μm. As the average diameter of mammalian cells is approximately 10 μm [4], each node contains about 10 cells. We assume that the glucose concentration in the vessel is the normal glucose concentration in human sera—i.e., 5.5 mM [15]. The diffusion coefficient of glucose in MTSs varies from 8.3×10^{-4} to 2.0×10^{-3} cm^2/h [16]. For this reason, we take $\alpha' = 0.001$ cm^2/h.

Figure 5 of Ref. [17] shows a linear relation between the rate of glucose consumption and the average cell volume. If we take a linear approximation for Eq. (1) and work with this data set, we obtain $\gamma_{as} \approx 200$/h. The metabolic rate of glucose consumption was measured as a function of tumor grade in Ref. [18]. Using the results of this experiment, we may assume that the cancer cells consume 80 μmol/(100 g tissue min) and, proceeding in the same way as for γ_{as}, we propose $\beta_{as} \approx 5$/h. The migration coefficient values have a wide range of variation, from 2.5×10^{-8} to 5.4×10^{-5} cm^2/h, for cancer cells [19,20]. In general, we choose $\alpha = 8.3 \times 10^{-8}$ cm^2/h, which is near the low end of the range, because we also want to know if the tumor arrives to latency.

On the basis of many runs the temporal discretization was chosen to be $\tau = 0.001$ h. Cell growth and division are regulated by the cell cycle. The cell-cycle duration is approximately 12 h in exponentially growing monolayer cultures [5]. Therefore, we inspect the threshold Q_M every 12 000 steps. We also inspect the thresholds P_D and Q_D every 12 000 steps. Table I summarizes the reference values of the parameters used in the simulations. The constants P_D, r_M and r_D are taken to be equal to 2.61 mM, 1, and 0.25, respectively.

TABLE I. Numerical values of computational parameters.

Symbol	Unit	Value	References
ℓ	μm	33	
τ	h	0.001	
P_0	Mm	5.5	[15]
α'	cm^2/h	0.001	[5,16]
γ_0	1/h	0.002	[4,5]
γ_{as}	1/h	200	[4,17]
β_{as}	1/h	5	[18]
α	cm^2/h	8.3×10^{-8}	[19,20]

Initially the free nutrient distribution is stationary and the tissue is formed only by healthy cells. At $t = 0$ tumor growth starts from a cancer seed located at the center of the lattice. A large number of simulations have allowed us to identify to which parameters cancer growth is most sensitive. We have explored the effects of variations in these parameters, and here we report on the results obtained for the cases listed in Table II.

In general, the experimental data, such as tumor radius and viable rim thickness, are obtained from MTSs, which are three-dimensional (3D) culture cell systems with an approximately spherical shape and a concentrically layered structure. This structure consists of an inner necrotic core, an intermediate layer of viable but quiescent cells, and an outer shell of proliferating cells. In order to analyze our data we define the mean tumor radius as

$$R = \langle r \rangle = N^{-1} \sum_{i=1}^{N} r_i, \quad (5)$$

where N is the total number of nodes in the tumor edge and r_i is the distance from node point $\vec{i}$ to the center of mass of the tumor. In the same way we define the mean necrotic radius R_n. In this case N and r_i are, respectively, replaced by the number of nodes in the necrotic core-viable tumor zone

TABLE II. Parameters used for the simulations.

Name	α (cm^2/h)	γ_{as} (1/h)	β_{as} (1/h)	Q_M	Q_D	Symbol
(*A*)	8.3×10^{-8}	200	5	100	10	○
(*B*)	8.3×10^{-8}	200	5	40	10	+
(*C*)	8.3×10^{-8}	160	5	100	10	*
(*D*)	8.3×10^{-8}	250	5	100	10	△
(*E*)	8.3×10^{-8}	200	20	100	10	▽
(*F*)	8.3×10^{-8}	200	5	100	20	×
(*G*)	8.3×10^{-8}	200	5	150	10	□
(*H*)	8.3×10^{-8}	200	5	100	4	#
(*I*)	4.15×10^{-8}	200	5	100	10	⬡
(*J*)	16.6×10^{-8}	200	5	100	10	◇
(*K*)	2.5×10^{-8}	200	5	100	10	☆

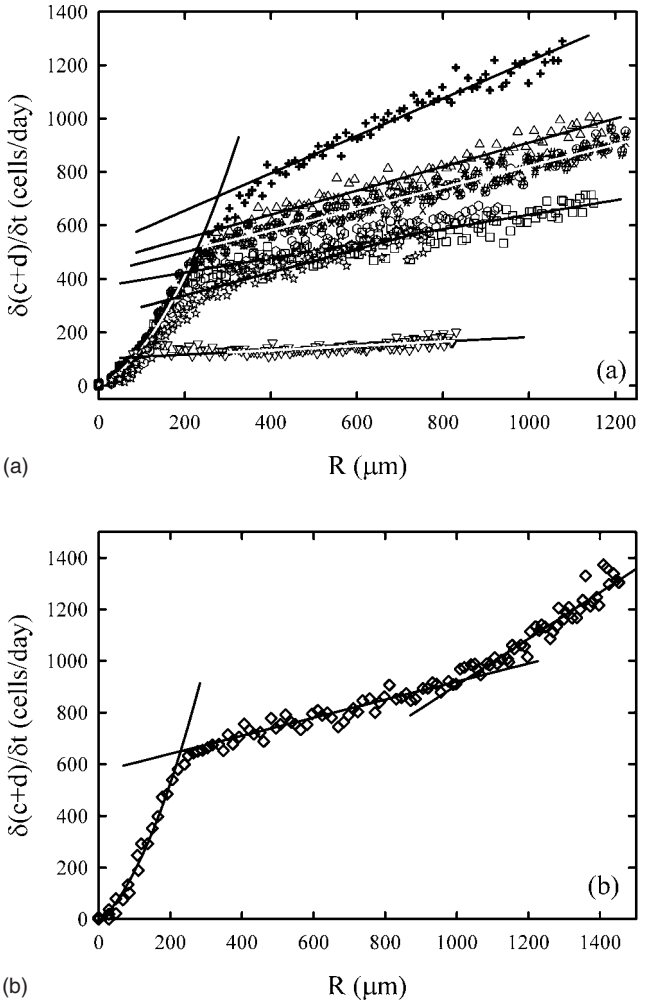

FIG. 1. Growth rates. (a) Simulation results for the cases detailed in Table II, except for case *J*, which is shown in panel (b). Symbols are for simulation results and solid lines are best fits.

interface and the distances of these nodal points to the center of mass of the necrotic core. We can associate the viable rim thickness Δ with the difference $R-R_n$.

If we want the cancer seed to thrive, it must be located in a region with a high concentration of glucose, which activates the cell cycle and induces cell proliferation. Therefore, when the tumor begins to grow all cancer cells are in a medium with a sufficient amount of nutrients to complete the cell cycle and there are no quiescent cells present. At these early times the growth rate is proportional to the number of tumor cells, which is itself proportional to R^2 for two-dimensional tumors. Therefore, the tumor mass m grows exponentially, because

$$\frac{dm}{dt} \propto \frac{dR^2}{dt} \propto R^2 \Rightarrow \frac{dR}{dt} \propto R. \tag{6}$$

Subsequently, the supply of nutrients gradually decreases due to the limited diffusivity of glucose, whose concentration falls in the central region, whose cells become either quiescent or necrotic. Since the proliferating cells are concentrated

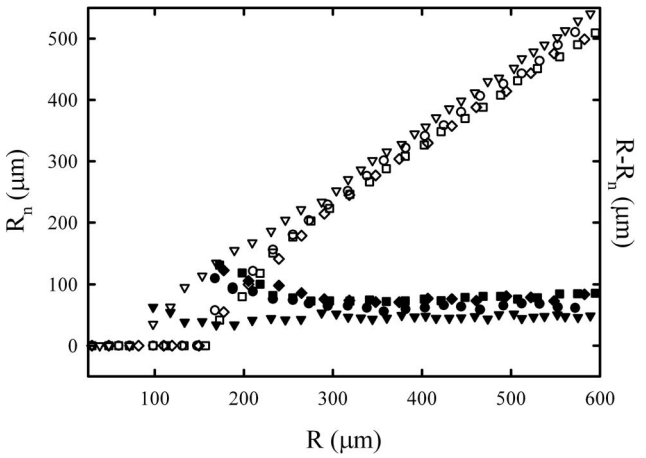

FIG. 2. Mean radius R_n (open symbols) of the necrotic region and viable rim thickness (solid symbols), as functions of the mean tumor radius R. Simulation parameters are those in Table II.

in the tumor periphery, the growth rate becomes proportional to R for two-dimensional tumors and

$$\frac{dm}{dt} \propto \frac{dR^2}{dt} \propto R \Rightarrow \frac{dR}{dt} = \text{const}. \tag{7}$$

This argument has been used by Brú *et al.* [21]. It is easy to see that the result $dR/dt=$const holds for 3D systems, too. Experimental evidence showing that the mean tumor radius grows linearly with time can be found in [17,21–23].

In Fig. 1 we show the evolution of the rate of change of the total number of cancer and dead cells, $\delta(c+d)/\delta t$, as a function of R, where $c=\Sigma_{\vec{i}} c(\vec{i})$ and $d=\Sigma_{\vec{i}} d(\vec{i})$. The results show good qualitative agreement with experimental data [17,21–23] and the theoretical predictions above. In all cases, there is a well-defined crossover between the exponential and linear regimes. The slope of the linear region is larger in those cases where the linear regime begins at larger sizes, the exception being curve *K*, which corresponds to a very low migration coefficient. The lowest curve corresponds to case *E*: the high consumption rate leads to slow growth, and the linear regime is reached for a small value of the radius. The uppermost curve corresponds to case *B*: the low mitosis threshold delays the crossover and leads to very fast growth. In case *J*, shown in Fig. 1(b), a second slope change takes place around $R=R_c=1050$ μm. This case corresponds to the highest value considered for the cell migration coefficient. According to rule (V) above, cell migration is activated when the free nutrient concentration near the cell is less than P_D, and therefore it is indirectly regulated by γ_{as}, β_{as}, and α'. Our simulations indicate that an increase in α becomes relevant for tumor sizes greater than a critical size defined by the depth of the nutrient depletion hole around the tumor. Above this critical size, cell migration is favored and cancer cells can explore regions with higher concentration of nutrients, leading to the observed increase in the growth rate for large tumors.

In Fig. 2 we show R_n and Δ as functions of R. We can see that the viable rim thickness remains approximately constant for different sets of parameters. This property is known ex-

perimentally [24,25]. The experimental data for Δ reported in these articles vary from 80 to 500 μm. Our results are smaller than the experimental values due to the two-dimensionality of the simulations. Although no qualitative differences are expected between the two- and three-dimensional results, the value of Δ is expected to be larger in three-dimensional systems because of the larger number of diffusion paths between any pair of node points. For clarity we just show some illustrative runs; for all the other runs considered, the results fall between the lowest and uppermost curves. For the lowest curve the necrosis starts earlier than for any other reported curve. Other simulations show that moving the seed towards the feeding vessel increases the number of cancer cells, but does not substantially alter the tumor shape.

In this work we used a mathematical model to describe cancer growth, finding that the hypotheses of the nutrient competition model necessarily lead to an initially exponential growth followed by a linear regime. We also showed that the viable outer layer of the tumor, formed by reproductive and quiescent cells, has an approximately constant thickness. Extensive simulations using realistic parameter values indicate that the transition to latency is never achieved. Indeed, we find that a phase transition occurs only if the diffusivity of the critical nutrient is much smaller than that of glucose in MTSs. Therefore, the observation that MTS diameters usually do not reach 2 mm indicates that an inhibitor (perhaps accumulated wastes [5]) must be at work. The presence of this inhibitor can explain the growth saturation usually described by the Gompertz law. The absence of latency is consistent with the intuitive idea that growth proceeds because cells in the outer tumor rim are always exposed to high nutrient concentrations. A geometric property that remains to be investigated is the roughness of the tumor surface, whose width has been predicted to increase as $|\ln(t)|^{1/2}$ [26].

This work was supported by SECyT-UNC (Project No. 05/B354), ANPCyT (Grant No. PICT 2205/33675), and CONICET (Grant No. PIP 6311/05).

[1] L. Preziosi, *Cancer Modeling and Simulation* (Chapman and Hall/CRC, London, 2003).
[2] S. C. Ferreira, M. L. Martins, and M. J. Vilela, Phys. Rev. E **65**, 021907 (2002).
[3] J. D. Nagy, Math. Biosci. Eng. **2**, 381 (2005).
[4] D. Drasdo and S. Hühme, Phys. Biol. **2**, 133 (2005).
[5] Y. Jiang, J. Pjesivac-Grbovic, C. Cantrell, and J. P. Freyer, Biophys. J. **89**, 3884 (2005).
[6] H. B. Frieboes, X. Zheng, Ch.-H. Sun, B. Tromberg, R. Gatenby, and V. Cristini, Cancer Res. **66**, 1597 (2006).
[7] M. Scalerandi, A. Romano, G. P. Pescarmona, P. P. Delsanto, and C. A. Condat, Phys. Rev. E **59**, 2206 (1999).
[8] P. P. Delsanto, A. Romano, M. Scalerandi, and G. P. Pescarmona, Phys. Rev. E **62**, 2547 (2000).
[9] M. Scalerandi, B. Capogrosso Sansone, C. Benati, and C. A. Condat, Phys. Rev. E **65**, 051918 (2002).
[10] B. Capogrosso Sansone, P. P. Delsanto, M. Magnano, and M. Scalerandi, Phys. Rev. E **64**, 021903 (2001).
[11] S. A. Menchón, R. A. Ramos, and C. A. Condat, Physica A **386**, 713 (2007).
[12] S. A. Menchón and C. A. Condat (unpublished).
[13] A. Brú, S. Albertos, J. A. Lopez García-Asenjo, and I. Brú, Phys. Rev. Lett. **92**, 238101 (2004).
[14] S. A. Menchón and C. A. Condat, Eur. Phys. J. Spec. Top. **143**, 89 (2007).
[15] J. Fang, M. Sullivan, and T. F. McCutchan, J. Biol. Chem. **279**, 720 (2004).
[16] J. J. Casciari, S. V. Sotirchos, and R. M. Sutherland, Cancer Res. **48**, 3905 (1988).
[17] J. P. Freyer and R. M. Sutherland, J. Cell Physiol. **124**, 516 (1985).
[18] A. C. Kole, B. E. C. Plaat, H. J. Hoekstra, W. Vaalburg, and W. M. Molenaar, J. Nucl. Med. **40**, 381 (1999).
[19] M. Chaplain and A. Matzavinos, *Tutorials in Mathematical Biosciences III: Cell Cycle, Proliferation, and Cancer* (Springer, New York, 2006), pp. 131–186.
[20] K. R. Swanson, C. Bridge, J. D. Murray, and E. C. Alvord, Jr., J. Neurol. Sci. **216**, 1 (2003).
[21] A. Brú, J. M. Pastor, I. Fernaud, I. Brú, S. Melle, and C. Berenguer, Phys. Rev. Lett. **81**, 4008 (1998).
[22] S. Günther, C. Ruhe, M. G. Derikito, G. Böse, H. Sauer, and M. Wartenberg, Cancer Lett. **250**, 25 (2007).
[23] A. Brú, S. Albertos, J. L. Subiza, J. López García-Asenjo, and I. Brú, Biophys. J. **85**, 2948 (2003).
[24] W. Mueller-Klieser, Crit. Rev. Oncol. Hematol. **36**, 123 (2000).
[25] J. P. Freyer and R. M. Sutherland, Cancer Res. **46**, 3504 (1986).
[26] C. Escudero, Phys. Rev. Lett. **100**, 116101 (2008).